

RESIDUAL STRESS IN RF MAGNETRON SPUTTERED ZnO THIN FILMS on GaP SUBSTRATES AND NANOWIRES

D. Buc^{1*}, J. Kovac¹, V. Kutis², J. Murin², M. Caplovicova³, J. Skrinariova¹, P. Novak⁴,
J. Novak⁵, S. Hasenörl⁵, E. Dobrocka⁵

¹ Institute of Electronics and Photonics, Slovak University of Technology in Bratislava, Ilkovicova 3, 81219 Bratislava, Slovakia
*e-mail: dalibor.buc@stuba.sk; jaroslav.kovac@stuba.sk; jaroslava.skrinariova@stuba.sk

² Institute of Automotive Mechatronics, Slovak University of Technology in Bratislava, Bratislava, Ilkovicova 3, 81219 Bratislava, Slovakia
e-mail: vladimir.kutis@stuba.sk; justin.murin@stuba.sk

³ Center STU for Nanodiagnostics, University Research Park, Slovak University of Technology in Bratislava, Vazovova 5, 81243 Bratislava, Slovakia
e-mail: maria.caplovicova@stuba.sk

⁴ Institute of Nuclear and Physical Engineering, Slovak University of Technology in Bratislava, Ilkovicova 3, 81219 Bratislava, Slovakia
e-mail: patrik.novak@stuba.sk

⁵ Institute of Electrical Engineering, Slovak Academy of Sciences, Dubravska cesta 9, 84104 Bratislava, Slovakia
e-mail: eleknova@savba.sk; elekhase@savba.sk; elekdobr@savba.sk

Key Words: *Core-shell GaP/ ZnO nanowires, RF magnetron sputtering, Residual stress, ANSYS*

Abstract. Core-shell nanowires are promising building elements of solar cells for advanced solar energy conversion. They are inexpensive since of the small amount of material needed and are efficient because of strong light absorption and rapid carrier collection. In this paper, we discuss the deposition of ZnO thin films on GaP substrate and GaP nanowires by RF magnetron sputtering and their influence on the structural properties in dependent on substrate tilting during the deposition. The main goal of this work is to find the optimal technology for deposition very thin ZnO films by RF magnetron sputtering with defined parameters to cover round GaP nanowires surface prepared by MOCVD technology. The SEM and TEM characterization showed that the ZnO shells fully covered the surface of the GaP-NWs from top to bottom if the substrates rotate. The effects of sputtering angle on surface roughness and morphology behaviors have been investigated by SEM. On the not rotated substrates we observed bending of NWs as a result of residual stress. XRD analysis confirmed compress stress in ZnO film on GaP substrate. The ZnO films with different morphology had the nominal thickness between 60 and 180 nm measured on planar GaP substrate and 60 and 80

nm on GaP nanowires, respectively. The influence of residual stress on the bending of GaP/ZnO NWs was evaluated using ANSYS software code, as well as compared with experimental observations.

1 INTRODUCTION

Zinc oxide (ZnO) is emerging as a multifunctional material for broad applications in blue and ultraviolet optoelectronic devices because of its direct and wide band gap of 3.4 eV and large exciton binding energy ~ 60 meV [1, 2]. Nanowire solar cells are promising devices for solar energy conversion because of the enhanced optical absorption on structured surfaces [3]. Conductive and transparent *n*-type ZnO thin films have significant commercial impact due to their use as transparent electrodes for flat panel displays, organic light emitting devices and in solar cells. ZnO *n*-type conductivity is relatively easy to realize via Zn excess or with Al or Ga doping. The next improvement will be obtained by the preparation of a GaP-ZnO heterojunction and its application will allow the designer to shift the absorption edge more to the blue part of the solar spectrum [4]. GLAD (glancing angle deposition) is a versatile tool for preparation of unique 3D nanostructures with plenty of different morphologies on smooth or nanostructured surfaces [5]. In this paper, we discuss the effect of deposition of ZnO:Al conductive thin films by reactive magnetron sputtering on the tilted and rotated substrates with and without GaP-NWs, and their influence on the film morphology and structure. We proposed the model of the core/shell nanowire system on the basis of experimental measurements of the nanowire dimensions using SEM and TEM methods and material constants of GaP and ZnO. We simulated the influence of residual stress on the bending of GaP/ZnO NWs. ANSYS method provided the values of residual stress at the GaP/ZnO boundary and confirmed its applicability in the nano-dimensional modeling.

2 EXPERIMENTAL

The GaP nanowires were prepared in an AIX 200 MOCVD low-pressure reactor by a vapor-liquid-solid (VLS) method from 30 nm BBI colloidal gold particles. The Au particles were randomly distributed over the substrate at a density of $\sim 2 \times 10^8$ cm⁻². Nanowires deposition was performed in palladium purified H₂ carrier gas from phosphine (PH₃) and trimethylgallium (TMGa) used as the phosphorus and gallium sources, respectively [5] and provides the continued growth of nanowires with an extremely high length to diameter ratio (60 - 80). ZnO *n*-type conductivity thin films were next deposited on GaP substrate and GaP substrate with NWs by using RF reactive magnetron sputtering at room temperature (RT). The method has an advantage in low temperature flow from magnetron discharge. A sintered disk of ZnO:Al (of 99.99 % purity for both ZnO and Al₂O₃) with 2 at. % Al₂O₃ was used as a target. The diameter and the thickness of the target were 76 mm and 5 mm, respectively. Sputtering was carried out in on-axis target-substrate geometry. Based on previous experiences with ZnO deposition the new concept of tilted and rotated substrate holder was designed. The distance of substrate and target center was fixed at 60 mm, while central axes of the sample and target was tilted under angle φ , see Fig. 1. Substrates with GaP-NWs were placed on the rotating substrate holder with tilting arrangement. Within our deposition we used tilting angles φ of 82°, 65°, 45°, and 0°. The vacuum chamber was evacuated to a base pressure of $2 \cdot 10^{-3}$ Pa before sputtering. Then high-purity Ar and O₂ (99.999 % purity for both gases) were introduced as sputtering gas and reactive species, respectively. The total pressure was fixed at 0.15 Pa. The Ar/O₂ partial pressure ratio was set up to be equal to 15:1. Prior to

film deposition, the target was pre-sputtered for about 10 minutes to remove the surface contaminants. The films were deposited on substrates at 13.56 MHz at a power of 125 W. ZnO films were sputtered at room temperature with a sputtering rate of ~10 nm/min and their thickness on GaP substrates was determined by Dektak 150 instrument. This new concept allowed studying the influence of different tilting angle on the film morphology and structure.

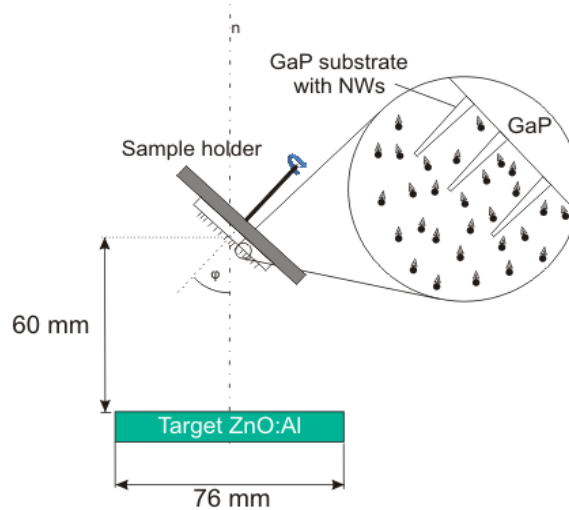


Fig. 1: Geometry of magnetron sputtering arrangement

The rotation speed was 40 rev/min. The characterization of GaP-NWs was made by employing two methods: The thickness of the deposited ZnO layer was determined in SEM observation by using the subtraction of the NW radius before and after magnetron deposition of ZnO layer. The second way consisted of the withdrawal of the individual nanowires to the microscopic TEM grid equipped with membrane and their measurement in TEM. The surface morphologies of ZnO films and core-shell GaP/ZnO NWs were examined by AFM (Veeco, Di CP-II.), SEM (FE-SEM Hitachi S-4300), TEM (transmission electron microscopes JEOL JEM 2000 FX equipped with the ASID20 scanning unit and JEOL JEM 200CX working at accelerating voltages of 160 and 200 kV, respectively). For defining the boundary layer of GaP/ZnO-NW, we utilized the contrast arising in the TEM diffraction. For TEM observations, GaP-NWs were fixed onto TEM Cu-grid covered by collodium and carbon layer and then examined using electron microscope.

2 RESULTS AND DISCUSSION

2.1 SEM

In general, the crack occurrence in a film is usually caused by substrate, composition, thickness, and thermal annealing conditions. In this study, the SEM micrograph reveals that ZnO films grown on GaP-NWs and GaP (111) substrate were uniform and crack free, which could be related to a precise stoichiometry ratio in ZnO films with a thickness of about 100 to 200 nm. Evolution of the surface microstructure of the ZnO thin films deposited on GaP

substrates was observed using SEM. The SEM micrographs of the GaP-NWs after their MOCVD growth and after magnetron sputtering of ZnO shell are shown in Fig. 2. The as-grown nanowires are typically $\sim 4 - 6 \mu\text{m}$ long and $50-80 \text{ nm}$ in diameter shown in Fig. 2a. The ZnO shells were deposited on the nanowire surface with different side thickness $\sim 20-100 \text{ nm}$. The polycrystalline ZnO layers showed good homogeneity of the grains ordering with $\sim 10 \text{ nm}$ grain height and $\sim 50-80 \text{ nm}$ grain diameter.

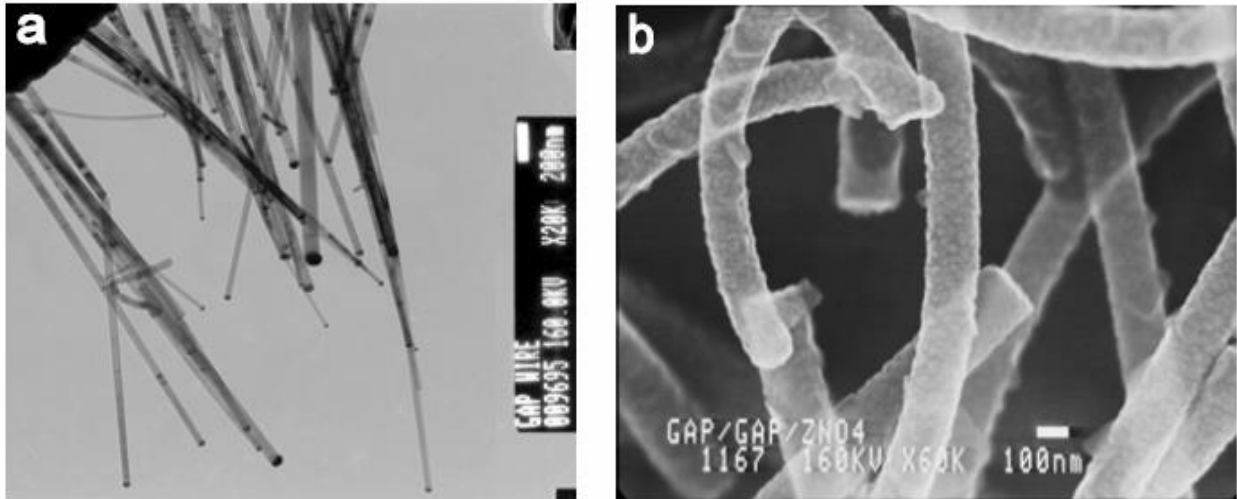


Fig. 2: a) Bright field TEM image of group of GaP-NWs cluster after their MOCVD growth and b) SEM image of GaP-NWs with deposited ZnO:Al layer at $\varphi = 82^\circ$ without substrate rotation

In comparing the SEM micrographs of Fig. 3 the tilting angle and rotation plays a major role by covering and bending the NWs during the deposition. The bending of covered NWs is always present without rotation of the substrate as shown in Fig 2b. On the other hand, by the rotation of the substrate the bending is minimized as evident from Fig. 3(a-f) and small bending is caused due to location of the substrate out of centre. For the next series of samples the substrate was centred in the middle of rotating holder and different alignment of the deposition tilting angle in the range of $0 - 82^\circ$. This new concept allowed studying the influence of different tilting angle on the film morphology and structure while at the same sputtering rate of $\sim 10 \text{ nm/min}$ and time. In Fig. 3(a-c) the SEM micrograph of a GaP-NWs covered by ZnO film at tilting angle 82° revealed that the ZnO film is uniformly covered over the GaP-NW and no bending occurs. The surface morphology of ZnO film shows polycrystalline structure with homogenous grain formations $\sim 30-40 \text{ nm}$ and determined thickness $\sim 60 \text{ nm}$.

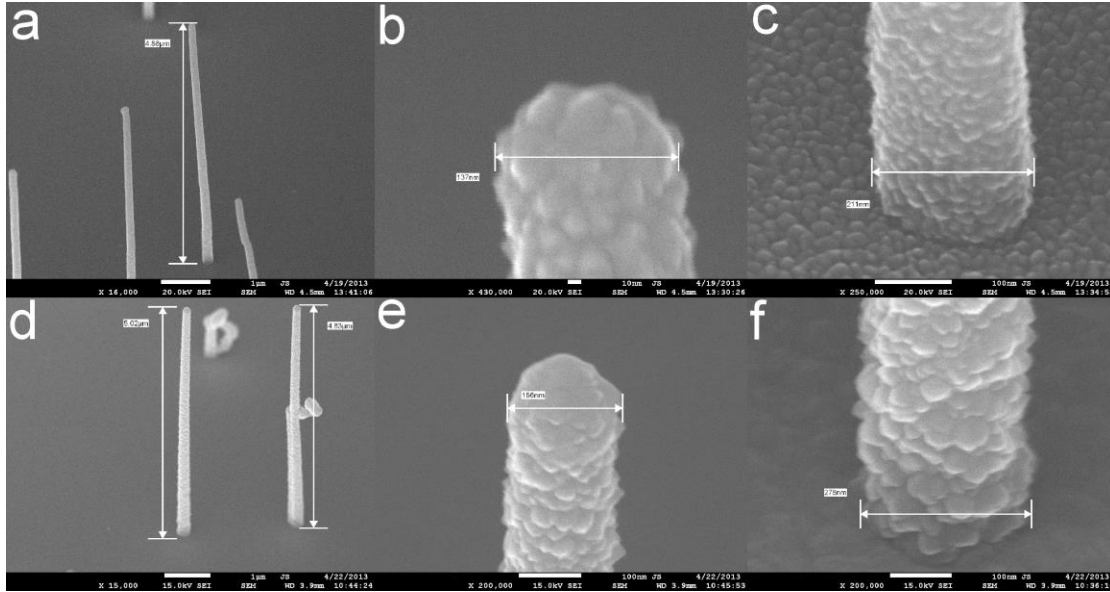


Fig. 3: (a,b,c) are SEM micrographs of a GaP-NWs covered in ~60 nm thick ZnO film. Tilting angle was 82° , rotating substrate, time 30 min; (d,e,f) are SEM micrographs of a GaP-NWs covered in ~60 nm ZnO film. Tilting angle ϕ was 0° , rotating substrate, time 30 min

The change of tilting angle ϕ up to perpendicular deposition (0°) gradually changed the formation of ZnO film morphology as shown in Fig. 3(d-f). The surface morphology of ZnO film shows polycrystalline structure with increased grains formations as flakes ~ 50-60 nm and determined thickness ~90 nm.

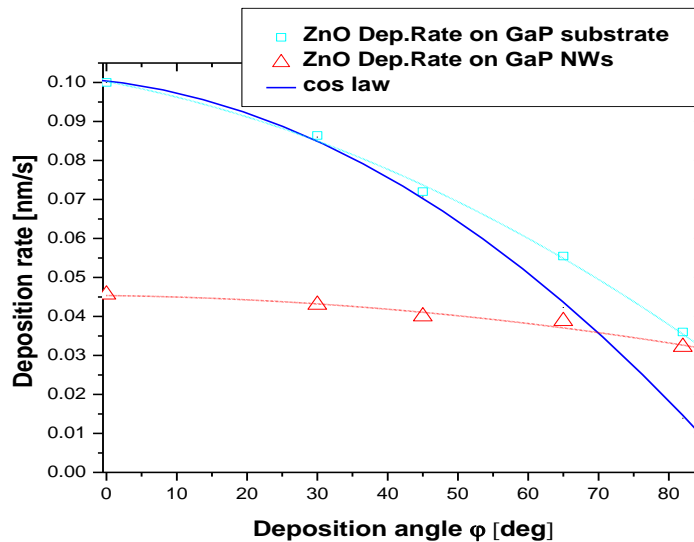


Fig. 4: Dependence of ZnO film thickness as a function of deposition angle α . ZnO film deposited on GaP-NW and GaP (111) substrate

Thickness dependence as a function of deposition angle ϕ for all investigated samples and for GaP-NWs and GaP (111) substrate prepared at the same deposition conditions, is shown in Fig.4. We can see the decreased tendency of the film thickness with deposition angle ϕ , while the thickness of ZnO films on GaP-NWs is 1 to 2 times lower in comparing with GaP substrates. These investigations confirmed the importance to control the ZnO film thickness directly on GaP-NW.

2.2 XRD

XRD data of ZnO films on GaP (111) substrates deposited by using of different tilting angles at reactive magnetron sputtering are shown in Fig. 5. The spectra show a strong preferential (002) orientation and (103) reflections of the wurtzite ZnO structure and are detected in all cases of our sputtering arrangements. The X-ray diffraction patterns for stress evaluation were measured in grazing incidence set-up, Fig. 5. In order to determine the changes of the strain and the stress with depth, three values for the angle of incidence α were chosen, 3° , 1.5° and 0.3° . The critical angle α_c for total external reflection of X-rays for crystalline ZnO is 0.332° . For $\alpha = 3^\circ$ and 0.3° the penetration depths $z_{1/e}$ for ZnO are 196 and 4.5 nm, respectively, i. e. at 3° the X-ray beam penetrates the whole volume of the 140 nm thick layer, while at 0.3° the gain of the information is restricted to the topmost layer with the thickness less than ~ 5 nm. The stress was evaluated by multi-reflection method [6] with correction for the refraction of X-rays. The layers of polycrystalline ZnO deposited on (111) oriented GaP substrates exhibit strong (002) texture without any pronounced azimuthal dependence as it is shown in Fig. 5. Due to this texture only three reflections (002, 103, 203) with sufficient intensities could be used for stress evaluation. The in-plane strain components ϵ^{II} of the 140 nm thick layer were determined as -0.020 and -0.015 for $\alpha = 3^\circ$ and 0.3° , respectively. The reference lattice parameters of the bulk ZnO were taken from PDF No. 36-1451 [7].

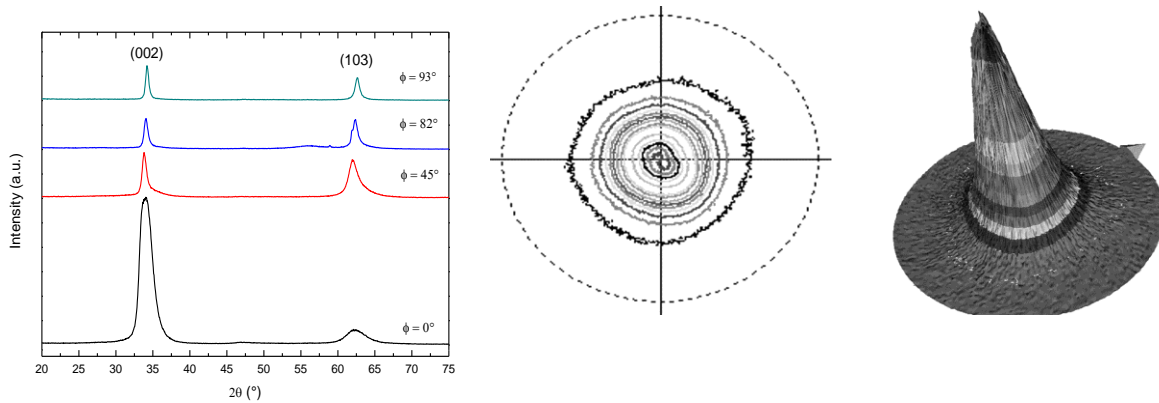


Fig. 5: Grazing incidence X-ray diffraction patterns of the ZnO layers (left) deposited at different tilting angles. The X-ray incidence angle was $\alpha=1.5^\circ$. Pole figure 002 (middle) and the corresponding 3D view (right) of the textured ZnO layer deposited at the tilting angle 82°

These values clearly show that the strain at the surface of the layer strongly decreases and reaches about 75% of the value averaged across the whole layer thickness. The corresponding values of compressive stress are 1.7 and 1.3 GPa, resp., when the isotropic stress factor

$E/(1+\nu) = 86.1$ GPa [8] is used. Distribution function of crystallite orientation is defined by the reference spherical area and pole figure is a projection of this area to the plane. Middle of the pole figure corresponds to the surface normal of the sample and consequently planes (002) are parallel to the sample surface.

2.3 TEM

TEM images of a GaP/ZnO nanowires revealed that GaP nanowire has zinc blende crystal structure and growth axis [111] and the structure of the ZnO shell is polycrystalline (Fig. 6). We observed bending of the NWs after deposition of shell ZnO layer on fixed positioned NWs without the rotating the substrate with NWs as a result of the residual stress in the ZnO polycrystalline coating. On the Fig. 6b we can observe two different thickness of ZnO shell on adjacent and adverse side of GaP-NW.

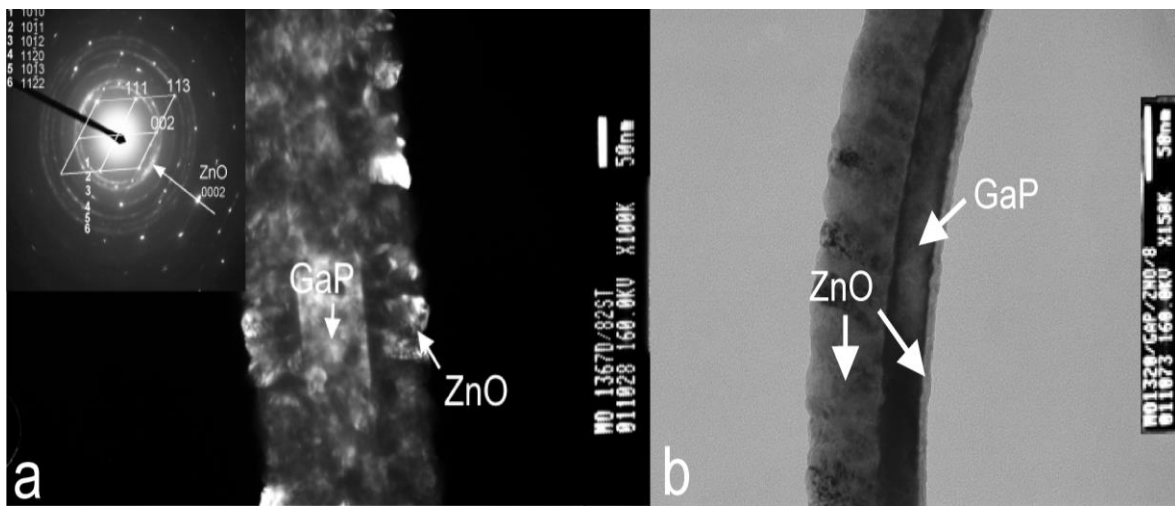


Fig. 6: TEM images of as grown GaP/ZnO NW deposited with tilting angle a) $\varphi = 82^\circ$ with rotation. (Inset shows diffraction analysis of the sample); b) the same angle without rotation

There are two main streams of depositing particles in the sputtering process: 1) direct stream, comprising the target particles flying from the target after their sputtering and 2) indirect stream, whose origin arises from the scattering process of the sputtered particles by their collisions with gas molecules, Fig.1. Deposition of the thin ZnO film of about 10 nm, measured on the GaP surface of the reversed side of the nanowire, viewing from the direction from the particle source, is caused by the indirect stream, see Fig.6b.

2.4 ANSYS MODELING AND SIMULATION

We simulated the influence of residual stress on bending of GaP/ZnO NWs using ANSYS software code. With the aim to show distribution of the stress along GaP/ZnO core/shell NW, we have utilized a simplified model shown in the Fig. 7. Geometrical parameters were chosen according to grown GaP nanowires observed using a field-emission scanning electron microscope. After measurements of the geometric dimensions of the NWs, these values were rounded and included in the NW modeling all at once by applying the material parameters in Tab. 1.

Tab. 1: Measured dimension of GaP/ZnO nanowires used in ANSYS [9] calculations

GaP dia. at fixed end	D_1	90 nm
GaP dia. at free end	D_2	35 nm
ZnO dia. at free end	D_3	55 nm
NW length	L	5 μm
Height	h	145 nm
ZnO bottom radius	R_1	55 nm
ZnO upper radius	R_2	150 nm
Deflection	y_{max}	3 μm

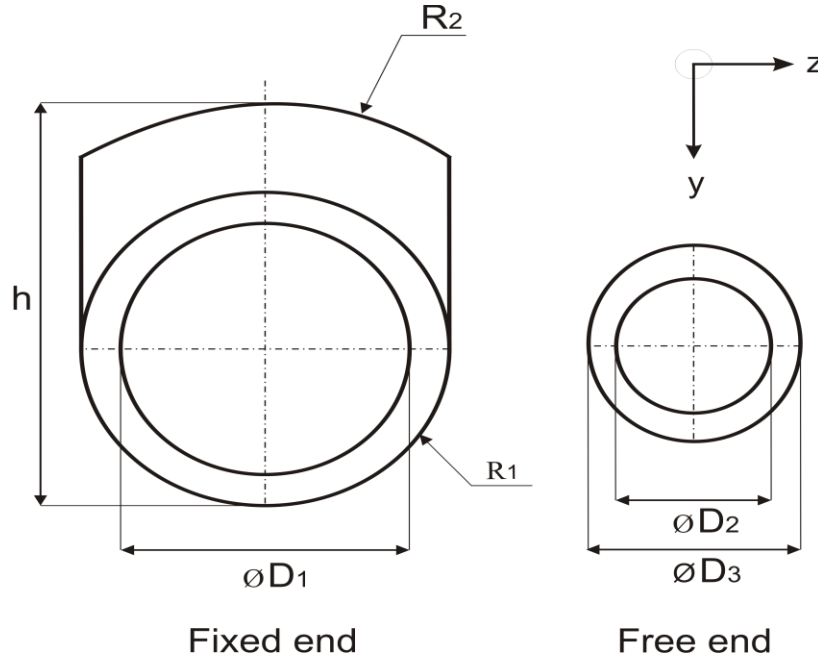


Fig. 7: Schematics of the GaP/ZnO NW cross-section

Tab. 2: Material properties of GaP and ZnO used in ANSYS calculations

Material properties		GaP	ZnO
Young's modulus	E [GPa]	103	112
Poisson's ratio	ν [-]	0.31	0.3
Yield strength	σ_p [MPa]	600	450

The GaP and ZnO material properties are listed in Tab. 2 based on [10-12]. Note, however, that some authors e.g. [13,14] use a significantly different value of the GaP's Young modulus.

For numerical simulation of residual stress in GaP/ZnO, nanowire FEM code ANSYS (total number of over 1.3 million elements) was utilized. Since the cross-section of nanowire is varying along the nanowire length, solid element type SOLID 185 was used. Bottom part of model was fixed and only the symmetrical part of the nanowire was considered. Because expected deformation of model is relatively large, the quality of mesh could have a strong influence on obtained results and therefore structured mesh was used. The residual stress induced by lattice mismatch was modeled by utilizing artificial thermal expansion, which was set to ZnO layer.

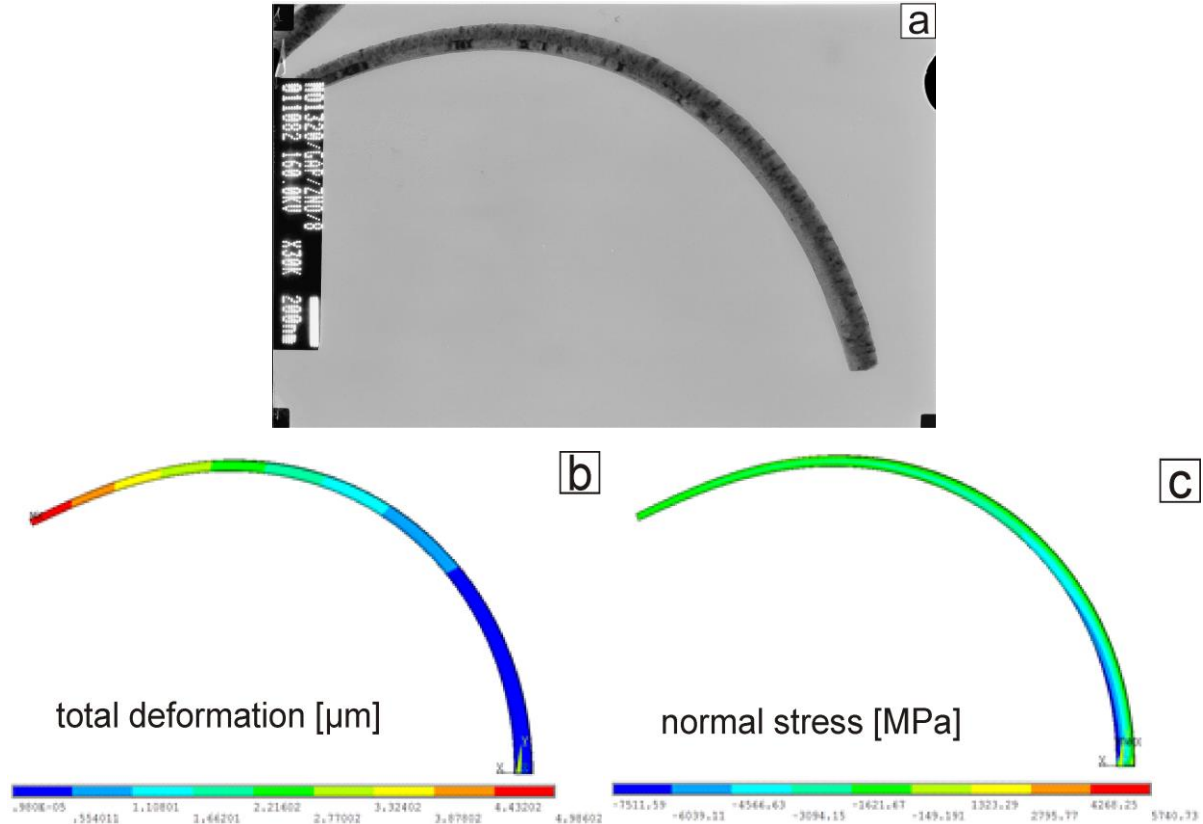


Fig. 8: (a) Bended nanowire as observed by TEM, (b) total deformation and (c) distribution of normal stress in longitudinal direction of the bended NW as a result of the numerical analysis

Artificial thermal expansion coefficient, together with prescribed artificial temperature difference between actual and reference state, defined the deformation of the model and these two parameters were set up so that state match to deformation of measured nanowire, Fig. 9. A comparison of a real sample from the experiment and modeling result is shown in Figs. 8, 9. As we can see from obtained numerical results, the distribution of normal stress near the fixed end is strongly influenced by this boundary condition. Figures show not only distribution of normal stress in individual cross-sections but also dependence of normal stress on location from left to the right (denoted as point 1 - left and point 2 - right). The stress-strain analysis revealed that the stress in the ZnO shell on GaP core nanowire in his middle part is in the range from compressive to tensile from ~ -3.1 to 2 GPa. The stress in the system GaP/ZnO-NW in the thicker end is changing in the direction from the inner part of the bended

NW (compressive) to the GaP center (tensile). Stress is released along the nanowire from the thicker end to the thinner one. This can be attributed to the fact that the mechanical properties of both materials are almost identical, hence the nanowire behaves like a solid rod subjected to a bending moment. The calculated values of normal stress are also lower than denoted values common for rf magnetron sputtered ZnO films [15]. This difference is a consequence of the low toughness of the subtly GaP-NWs in comparison with mechanically inflexible monocrystalline substrate. The bending curve is, as expected, affected by the change in the cross-section throughout the NW's length.

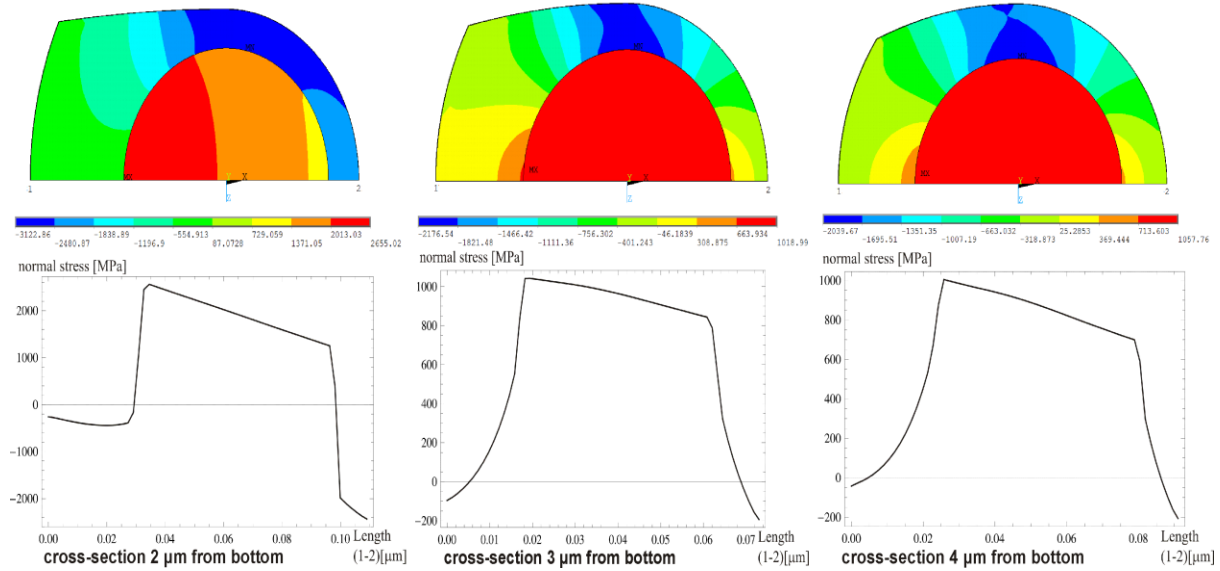


Fig.9: The distribution of normal stress in three different cross-sections (2, 3 and 4) μm from fixed end of the model

3 CONCLUSIONS

Significant research effort is underway on ZnO nanostructures due to their unique properties for application in transparent electronics, photovoltaics, ultraviolet light emitters, piezoelectric devices, chemical sensors and spin electronics. Our investigations allowed finding the optimal technology for deposition of very thin ZnO films of the different morphology to cover cylindrical GaP nanowire surface using MOCVD technology. In this paper, we have discussed growth conditions and characterization of ZnO polycrystalline films deposited by RF magnetron sputtering on GaP substrates and core-shell GaP/ZnO nanowires. A homogeneous microstructure having a uniform grain size and different morphology could be observed at room temperature growth of ZnO films by placing the substrate in the middle of rotating holder and changing alignment of the deposition angle in the range of 0 – 82°. SEM and TEM investigations enabled to determine the thickness of deposited ZnO film on GaP-NWs as well as their structure morphology. XRD measurements confirmed the internal compressive residual stress which bends the GaP/ZnO core/shell NWs along the downstream direction of bombarding particles. We created the model of GaP/ZnO nanowire and simulated the influence of residual stress on the bending of GaP/ZnO NWs. ANSYS method provided the values of residual stress at the GaP/ZnO boundary and confirmed its applicability in the

nano-dimensional modeling. The oblique angle reactive magnetron sputtering which combines the substrate tilting angle with and/or without rotation offers a flexible tool for the deposition of the homogenous coatings with improved properties.

ACKNOWLEDGEMENT

The work was supported by by the Slovak Research and Development Agency under the contracts APVV-0246-12, grant of Science and Technology Assistance Agency “GRONA” no. APVV-0301-10 and VEGA projects 1/1106/12, 1/0228/14, 1/0439/13, 1/0534/12, 2/0147/11.

REFERENCES

- [1] H. Xu, X. Liu, D. Cui, M. Li, M. Jiang, *Sensors and Actuators B*: (2006) **114**: 301.
- [2] A. Strohm, L. Eisenmann, R. K. Gebhardt, A. Harding, T. Schlftzer, D. Abou-Ras, H. W. Schock, *Thin Solid Films* (2005) **480–481**: 162.
- [3] P. W. Bao, Ch. Z. Zhao, Z. Neng, *Solid State Sciences* (2010) **12**:1188.
- [4] S. Hasenöhr, P. Eliáš, I. Vávra, I. Novotný, J. Kováč, J. Novák, XIV European Workshop on Metalorganic Vapor Phase Epitaxy EW-MOVPE (2011), June 5-8, Wrocław, Poland, p. 259-262.
- [5] K. Robbie, G. Beydaghyan, T. Brown, C. Dean, J. Adams, C. Buzea, *Review of Scientific Instruments* (2004) **4 75**: 1089.
- [6] A. Baczmanski, C. Braham, W. Seiler, N. Shiraki, *Surface and Coating Technology* (2004) **182**: 43.
- [7] Powder Diffraction File, JCPDS, 1967, ASTM, Philadelphia, PA 1967, No. 36-1451.
- [8] Zinc Oxide: Fundamentals, Materials and Device Technology. Hadis Morkoç and Ümit Özgür, WILEY-VCH Verlag GmbH & Co. KGaA, Weinheim, 2009.
- [9] ANSYS Swanson Analysis System, Inc., 201 Johnson Road, Houston, PA 15342/1300, USA.
- [10] Wen-Jay Lee, Structure-dependent mechanical properties of ultrathin zinc oxide nanowires, *Nanoscale Research Letters* (2011) **6**: 352.
- [11] Li Qiao et al., Effect of surface stress on the stiffness of micro/nanocantilevers: Nanowire elastic modulus measured by nano-scale tensile and vibrational techniques, *Journal of Physics D Applied Physics*, (2013) **113**: 013508.
- [12] S. Hasenöhr, P. Eliáš, J. Šoltýs, R. Stoklas, A. Dujavová, J. Novák, Zinc-doped gallium phosphide nanowires for photovoltaic structures. In: *Applied Surface Science* (2013) **269**: 72-76, ISSN 0169-4332.
- [13] Woong Lee, Min-Chang Jeong and Jae-Min Myoung, Fabrication and application potential of ZnO nanowires grown on GaAs(002) substrates by metal–organic chemical vapour deposition, *Nanotechnology* (2004) **15**: 254-259.
- [14] Guangyin Jing, Xinzheng Zhang, Dapeng Yu, Effect of surface morphology on the mechanical properties of ZnO Nanowires, *Appl Phys A* (2010) **100**: 473–478, DOI 10.1007/s00339-010-5736-7.
- [15] G. Anil Kumar, M. V. Ramana Reddy and Katta Narasimha Reddy, Effect of annealing on ZnO thin films grown on quartz substrate by RF magnetron sputtering. *International Conference on Recent Trends in Physics (ICRTP 2012)*, *Journal of Physics: Conference Series* 365 (2012) 012031.